A Sheaf and Topology Approach to Detecting Local Merging Relations in Digital Images

Chuan-Shen Hu
Department of Mathematics
National Taiwan Normal University
Taipei 116325, Taiwan
80547002S@ntnu.edu.tw

Yu-Min Chung
Department of Mathematics and Statistics
University of North Carolina at Greensboro
Greensboro, North Carolina 27412, USA
y_chung2@uncg.edu

Abstract

This paper concerns a theoretical approach that combines topological data analysis (TDA) and sheaf theory. Topological data analysis, a rising field in mathematics and computer science, concerns the shape of the data and has been proven effective in many scientific disciplines. Sheaf theory, a mathematics subject in algebraic geometry, provides a framework for describing the local consistency in geometric objects. Persistent homology (PH) is one of the main driving forces in TDA, and the idea is to track changes in geometric objects at different scales. The persistence diagram (PD) summarizes the information of PH in the form of a multi-set. While PD provides useful information about the underlying objects, it lacks fine relations about the local consistency of specific pairs of generators in PD, such as the merging relation between two connected components in the PH. The sheaf structure provides a novel point of view for describing the merging relation of local objects in PH. It is the goal of this paper to establish a theoretic framework that utilizes the sheaf theory to uncover finer information from the PH. We also show that the proposed theory can be applied to identify the merging relations of local objects in digital images.

1. Introduction

Topological data analysis (TDA) is a branch of applied mathematics that aims to quantify topological characteristics, especially the q-dimensional Betti numbers denoted by β_q. For instance, β_0, β_1, and β_2 represent the number of components, holes, or voids, respectively. *Persistent homology* (PH), one of the main tools in TDA, tracks changes of towered topological spaces induced by the original objects [27, 21, 15, 25, 49, 6]. Figure 2 (a) shows two examples of included spaces (also known as *filtrations*) of black regions. The q-dimensional PH of *filtration*[1] of topological spaces is a sequence of vector spaces that are connected by linear transformations[2]. The non-negative integer q denotes the dimension of objects which are captured by the PH. For instance, the PH of $q = 0$ captures the changes of connected components and $q = 1$ for holes in a filtration.

Persistence barcodes (or simply *barcodes*) are a typical way to summarize the information of PH. A barcode of a q-dimensional object/generator in PH is a pair of numbers (b, d) where the object/generator is born at the value b and dies at the value of d. One often refers to b, and d to the *birth* and *death*, respectively, values. For instance, in Figure 1, a 1-dimensional hole of the character "A" was born at g_2 and disappeared at g_4, and hence the hole has the barcode $(2, 4)$. Barcodes in PH can be defined rigorously as the algebraic structure of PH [27, 21, 15, 25] (cf. Lemma 2.2.1). The collection of all barcodes of q-dimensional objects is called the *persistence diagram* (PD) [27, 21, 15, 25]. PD plays an essential role in the application and has widely applied and studied in computer vision [66, 9, 61], machine learning [14, 1, 44, 53], image/signal processing [67, 11], medical science [50, 46, 22, 7, 10], and physics [62, 5].

Although PD contains information about the changes of local objects, the reduction algorithm for obtaining Smith normal forms [26] of the connecting linear transformations would omit the merging relations of elements in PH. In other words, the PD is not enough for researchers who are interested in the merging behaviors of certain local objects. For example, the top and bottom panels of Figure 2 (a) show two different filtrations of binary images, but they share the same persistence diagram $\mathcal{P}_0$ as shown in Figure 2 (b). The merging relation between connected components in the third image is different: one connects diagonally while the other connects horizontally.

[1] A filtration of topological spaces is an inclusions $X_1 \subseteq X_2 \subseteq \cdots \subseteq X_n$ of topological spaces.

[2] In algebraic topology, one may also consider PH of modules and module homomorphisms.

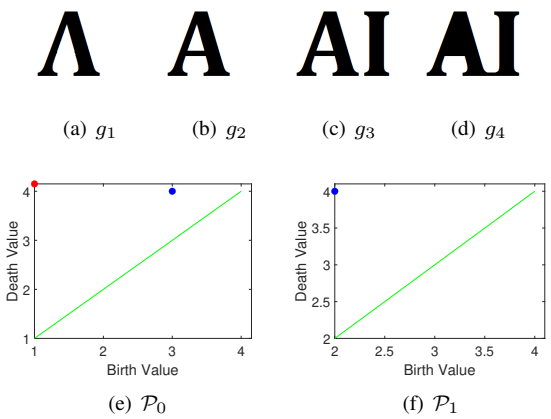

Figure 1. (a) $\sim$ (d) is a filtration of black pixels of binary images. (c) Binary image "AI", which has $\beta_0 = 2$ (connected components) and $\beta_1 = 1$ (1-dimensional holes). (e) and (f) are persistence diagrams $\mathcal{P}_0 = \{(1, \infty), (3, 4)\}$, $\mathcal{P}_1 = \{(2, 4)\}$ in dimension 0 and 1 of the filtration respectively.

There are some works related to the behaviors of local objects in PH, such as Mapper [42, 59] and local (co)homology [30, 29]. In particular, Vandaele *et al.* [64] investigated the local Vietoris-Rips complexes of point clouds. By computing the branch numbers b and the first Betti numbers β_1 of the induced graph structures, the pairs (b, β_1) correspond to the branch numbers and holes of local objects. The local pairs provide a heat map of branch numbers and loop structures. Comparing to the global Betti numbers, it is additional geometric information for the object. The proposed work bases on a similar idea and provides a sheaf theoretical approach to describe the local behaviors of a geometric object. Comparison of these two methods will be discussed at the end of Section 2.3.

Historically, sheaves were first developed as a tool for researching the nerve theory and fixed-point theorems [2, 28, 13], while the recent trend is to study algebraic geometry [36]. Sheaf theory and algebraic geometry provide fruitful results and tools in analyzing local/global properties of geometric objects, while the research of the combination of sheaves and TDA is still in its infancy. A sheaf $\mathscr{F}$ over a topological space X is a rule which assigns each open subset U of X to an algebraic object $\mathscr{F}(U)$. Except objects, a sheaf $\mathscr{F}$ also assigns each pair $V \subseteq U$ of open sets to a homomorphism $\rho_{UV} : \mathscr{F}(U) \to \mathscr{F}(V)$ as an connection between two algebraic objects. The assignments of U and $V \subseteq U$ are analogous to the space of functions on U and restriction of functions on V.

Recently, the combination of the sheaf theory and TDA has been found its potential in modeling and analyzing real data [31, 54, 56, 55, 8, 34, 24]. For example, Robinson [54] proved the Nyquist sampling theorem by computing cellular sheaf cohomologies on abstract simplicial complexes of real signals and their samplings. In the work, the concept of *global and local sections* on posets equipped with the *Alexandrov topology* [3, 4] is crucial for constructing the sheaf structures on digital/analog signals. Our work is also motivated by the *multi-parameter persistent homology* [20, 57, 35] and zigzag homology [16, 19, 18, 17]. The extension of barcodes to multi-parameter persistent homology is an active research area in TDA. As discussed in [39, 40, 24], sheaf theory may be an appropriate tool towards that goals. The cellular sheaves considered in the paper can be viewed as a form of zigzag homology and multi-parameter persistent homology. The proposed work aims to capture local sections of certain local objects and their geometric meaning in digital images.

Our main contributions can be summarized in the following.

- We propose the *coincidence* of pairs in the filtration of binary images. The coincidence can be identified as global/local sections of a sheaf of the form (6). When $q = 0$, the coincidence in a *short filtration* can be used to define *local merging numbers* as a heat map of each binary image.

- In the paper, we propose an approximation of local sections in a PH by its PD. The result allows practitioners to estimate the representatives of local objects in PH.

The organization of the paper is as follows. We present our main results in Section 2. The demonstration of generating local merging numbers of binary images is shown in Section 3. The discussions, future works, and the conclusion are in Section 4.

2. Cellular Sheaves Modeling

This section is separated into three parts. In Section 2.1, we briefly introduce the formal definition of *cellular sheaves over posets*. To define the local sections on cellular sheaves, the *Alexandrov Topology* and the $\mathfrak{B}$-sheaf are also mentioned. In order to be self-contained, we provide necessary notations and definitions. For further details on these topics, we refer readers to [24, 3, 4] and [47]. Theorem 2.2.2 in Section 2.2 approximates the local sections via barcodes. Finally, in Section 2.3, we apply our results to analyze local information of binary images.

2.1. Cellular Sheaves and Coincidence in PH

A *poset* (or partially ordered set) $(P, \leq)$ is a non-empty set P equipped with a relation $\leq$ on P which satisfies the following properties: Whenever $x, y, z \in P$, (1) $x \leq x$ (2) $x \leq y$ and $y \leq z$ implies $x \leq z$, and (3) $x \leq y$ and $y \leq x$ implies $x = y$.

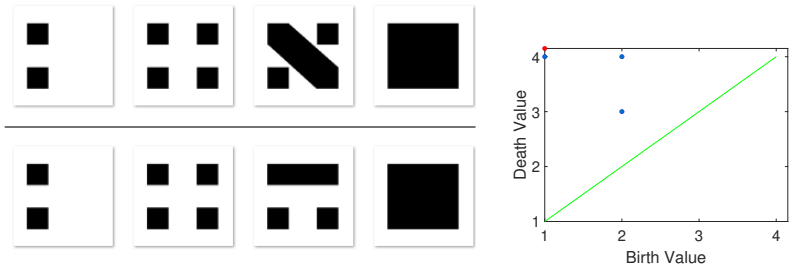

(a) Two filtrations of black pixels of binary images (b) The persistence diagram $\mathcal{P}_0$

Figure 2. An example of two filtrations of black pixels that share the same persistence diagram.

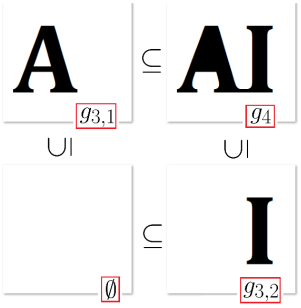

Figure 3. An example of inclusions separated from a filtration of binary images (cf. Figure 1 (a) $\sim$ (d)). These inclusion relations lead to the simplest cellular sheaf structure as in Equation (6)).

Example 2.1.1. *(1) Suppose X is a non-empty set and 2^X denotes its power set. Then the inclusion relation $\subseteq$ on 2^X is a partial order on 2^X. In this paper, we mainly consider $\subseteq$ on 2^S, where S is a subset of $\mathbb{Z}^2$.*
(2) Let $(x_1, x_2, ..., x_n), (y_1, y_2, ..., y_n) \in \mathbb{Z}^n$ be n-tuples over $\mathbb{Z}$. Define $(x_1, x_2, ..., x_n) \leq (y_1, y_2, ..., y_n)$ if and only if $x_i \leq y_i$ for all $i \in \{1, 2, ..., n\}$. Then $(\mathbb{Z}^n, \leq)$ is a poset.

A *cellular sheaf* over a poset $(P, \leq)$ is a rule which assigns each element in P to a vector space over a fixed field $\mathbb{F}$ (*e.g.* $\mathbb{Z}_2$ or $\mathbb{R}$) and preserves the ordering of elements in P via linear transformations. Here is the formal definition:

Definition ([55, 23]). *Let $(P, \leq)$ be a poset. A **celluar sheaf of vector spaces** (over a fixed field $\mathbb{F}$) on P is a rule $\mathscr{F}$ which consists of the following data:*

- *For each $p \in P$, $\mathscr{F}$ associates a vector space $\mathscr{F}(p)$ over $\mathbb{F}$.*
- *For $p \leq q$ in P, there is an $\mathbb{F}$-linear transformation $\rho_{p,q} : \mathscr{F}(p) \to \mathscr{F}(q)$ such that $\rho_{p,p}$ is the identity map on $\mathscr{F}(p)$ and $\rho_{q,r} \circ \rho_{p,q} = \rho_{p,r}$ for every $p \leq q \leq r$.*

In category theory, a cellular sheaf of vector spaces on a poset $(P, \leq)$ is a functor from the category of elements and partial relations in P to the category of vector spaces over a certain field [55, 23, 24]. By considering the *Alexandrov topology* [3, 4] $\mathfrak{A}$ on the poset P generated by the sets U_p's of forms

$$U_p = \{q \in P : p \leq q\} \tag{1}$$

as an open basis $\mathfrak{B}$ for the topology $\mathfrak{A}$, the assignment $U_p \mapsto \mathscr{F}(U_p) := \mathscr{F}(p)$ forms a $\mathfrak{B}$-sheaf structure on the topological space $(P, \mathfrak{A})$ [47]. The $\mathfrak{B}$-sheaf can be extended as a sheaf of vector spaces over $(P, \mathfrak{A})$, which is the real meaning of "sheaves on topological spaces"—from the aspect of traditional sheaf theory [13] or algebraic geometry [36, 47].

Because $\mathfrak{B} = \{U_p : p \in P\}$ is an open basis for $\mathfrak{A}$, every open subset U in $(P, \mathfrak{A})$ can be expressed by $U = \bigcup_{p \in U} U_p$. To extend $\mathscr{F}$ as a sheaf on $(P, \mathfrak{A})$, the $\mathscr{F}(U)$ is defined as the vector space

$$\mathscr{F}(U) = \{(s_p)_{p \in U} : s_q = \rho_{p,q}(s_p) \; \forall \; p \leq q\}, \tag{2}$$

where every $(s_p)_{p \in U}$ denotes an element in the Cartesian product $\prod_{p \in U} \mathscr{F}(p)$ of vector spaces [32, 54, 56, 24]. Elements in $\mathscr{F}(U)$ are called *local sections* on U, which are the most important targets for observing the coincidence of elements from different $\mathscr{F}(p)$'s. Here is an example:

Example 2.1.2. *Let $P = \{(0,0), (0,1), (1,0), (1,1)\}$ be a set of tuples in $\mathbb{Z}^2$. Then $(P, \leq)$ is a poset, where $\leq$ is defined as in Example 2.1.1 (2). Any cellular sheaf $\mathscr{F}$ on P can be represented as the commutative diagram*

$$\begin{array}{ccc} \mathscr{F}(0,1) & \xrightarrow{\rho_{(0,1),(1,1)}} & \mathscr{F}(1,1) \\ \uparrow{\scriptstyle \rho_{(0,0),(0,1)}} & & \uparrow{\scriptstyle \rho_{(1,0),(1,1)}} \\ \mathscr{F}(0,0) & \xrightarrow{\rho_{(0,0),(1,0)}} & \mathscr{F}(1,0) \end{array} \tag{3}$$

of vector spaces and linear transformations.

The local sections on $U := U_{(0,1)} \cup U_{(1,0)} = \{(0,1), (1,0), (1,1)\}$ are pairs (s,t) in $\mathscr{F}(0,1) \times \mathscr{F}(1,0)$ such that $\rho_{(0,1),(1,1)}(s) = \rho_{(1,0),(1,1)}(t)$ in $\mathscr{F}(1,1)$.

The concept of local sections described in Example 2.1.2 provides a bridge to investigate the relation between $\mathscr{F}(0,1)$ and $\mathscr{F}(1,0)$. A local section records elements s,t in $\mathscr{F}(0,1), \mathscr{F}(1,0)$ respectively, which would be identified as the same element in $\mathscr{F}(1,1)$ via $\rho_{\bullet,\bullet}$'s. More concrete examples for digital images and their sheaf structures are discussed in Section 2.3.

The cellular sheaf can be viewed as a generalization of persistent homology. For example, $\mathscr{F}$ in (3) is a 2-parameter persistent homology over the poset P. An one-parameter PH

$$H_q(X_0) \xrightarrow{\rho_{0,1}} H_q(X_1) \xrightarrow{\rho_{1,2}} \cdots \to H_q(X_n) \tag{4}$$

of topological spaces $\emptyset = X_0 \subseteq X_1 \subseteq \cdots \subseteq X_n$ is a cellular sheaf over $P = \{0,1,2,...,n\}$ of homologies and linear transformations[3] $\rho_{i,i+1} : H_q(X_i) \to H_q(X_{i+1})$ induced by the inclusions $X_i \hookrightarrow X_{i+1}$ [33], where

$$\rho_{i,j} := \rho_{j-1,j} \circ \cdots \circ \rho_{i,i+1} \tag{5}$$

and $\rho_{i,i}$ are the identity maps on $H_q(X_i)$ for $0 \le i < j \le n$.

Next we define the *coincidence of pair* $(s_i, s_j) \in H_q(X_i) \oplus H_q(X_j)$[4] to $H_q(X_k)$ with $i \le j \le k$ in (4). The motivation of the definition is to capture the merging relation between certain s_i and s_j in the filtration which can be viewed as a local version of the definition of barcodes (cf. Lemma 2.2.1).

Definition. *Let $\emptyset = X_0 \subseteq X_1 \subseteq X_2 \subseteq \cdots \subseteq X_n$ be a filtration of topological spaces and $0 \to H_q(X_1) \to H_q(X_2) \to \cdots \to H_q(X_n)$ be its PH. For $q \ge 0$, $i,j \in \{1,2,...,n\}$, $s_i \in H_q(X_i)$, $s_j \in H_q(X_j)$, and $\max\{i,j\} \le k \le n$, we say s_i and s_j **coincide** at k if $\rho_{i,k}(s_i) = \rho_{j,k}(s_j)$.*

In other words, if we extract $H_q(X_i)$, $H_q(X_j)$, and $H_q(X_k)$ from the PH, and consider natural linear transformations $H_q(X_i) \to H_q(X_k)$, $H_q(X_j) \to H_q(X_k)$[5], then the coincidence of pairs (s_i, s_j) can be regarded as the local sections in $H_q(X_i) \oplus H_q(X_j)$ with respect to the sheaf of form (3). This can be formulated as the following theorem.

Theorem 2.1.3. *Let $\emptyset = X_0 \subseteq X_1 \subseteq X_2 \subseteq \cdots \subseteq X_n$ be a filtration of topological spaces, $q \ge 0$, $s_i \in H_q(X_i)$, and $s_j \in H_q(X_j)$. Then s_i and s_j coincide at $k \ge \max\{i,j\}$ if and only if $(s_i, s_j) \in H_q(X_i) \oplus H_q(X_j)$ is a local section with respect to the cellular sheaf (6).*

$$\begin{array}{ccc} H_q(X_i) & \xrightarrow{\rho_{i,k}} & H_q(X_k) \\ & & \uparrow{\scriptstyle \rho_{j,k}} \\ & & H_q(X_j) \end{array} \tag{6}$$

[3] In the paper, we consider $H_q(X_i)$'s and $\rho_{i,i+1}$'s as vector spaces and linear transformations over the binary field $\mathbb{Z}_2$.

[4] For finitely many homologies, we use the notation $\oplus$ to replace $\times$.

[5] To emphasis the merging relation between s_i and s_j, here we ignore the linear transformation $H_q(X_i) \to H_q(X_j)$ for $i \le j$.

Proof. By the same arguments as in Example 2.1.2, an element $(s_i, s_j) \in H_q(X_i) \oplus H_q(X_j)$ is a local section of the cellular sheaf (6) if and only if $\rho_{i,k}(s_i) = \rho_{j,k}(s_j)$, as desired. □

For example, in the filtration (a) $\sim$ (d) in Figure 1, the component "I" has barcode $(3,4)$ since it was born at g_3 and finally be merged into "A". However, the persistence diagram (Figure 1 (e)) only shows that "I" has barcode $(3,4)$ while the merging information of "I" and "A" could not be concluded in the diagram.

As in Theorem 2.1.3, this local behavior between "A" and "I" is encoded as a local section of the cellular sheaf (7), by separating image g_3 into two parts $g_{3,1}$ = "A" and $g_{3,2}$ = "I". The inclusions $g_{3,1}^{-1}(0) \hookrightarrow g_4^{-1}(0)$ and $g_{3,2}^{-1}(0) \hookrightarrow g_4^{-1}(0)$ in Figure 3 lead the diagram

$$\begin{array}{ccc} H_0(g_{3,1}^{-1}(0)) & \xrightarrow{\rho_1} & H_0(g_4^{-1}(0)) \\ & & \uparrow{\scriptstyle \rho_2} \\ & & H_0(g_{3,2}^{-1}(0)) \end{array} \tag{7}$$

of 0-dimensional homologies where ρ_1 and ρ_2 are linear transformations induced by inclusions. Note that

$$\begin{aligned} H_0(g_{3,1}^{-1}(0)) &= \mathrm{span}_{\mathbb{Z}_2}\{\text{"A"}\}, \\ H_0(g_{3,2}^{-1}(0)) &= \mathrm{span}_{\mathbb{Z}_2}\{\text{"I"}\} \end{aligned} \tag{8}$$

and $\rho_1(\text{"A"}) = \rho_2(\text{"I"})$ in $H_0(g_4^{-1}(0))$. That is, the pair ("A", "I") is a local section which records that "A" and "I" finally merged into the unique connected component of g_4.

2.2. Approximation for Local Sections

Although elements in homology $H_\bullet(X)$ can be defined precisely (even discretely with $\mathbb{Z}_2$ as the field of coefficients), it is still difficult to represent elements in $H_\bullet(X)$ by comparing all representatives. To tackle this, we propose a method that uses barcodes of PH to approximate the local sections.

Here we recall the definition of barcodes of elements in PH [26]: let $\emptyset = X_0 \subseteq X_1 \subseteq \cdots \subseteq X_n$ be a filtration of topological spaces and $\{0\} \to H_q(X_1) \to \cdots \to H_q(X_n)$ be its PH, an element $s_i \in H_q(X_i)$ $(i \ge 1)$ is said to have *barcodes* (i,j) with $i < j$ if it satisfies the following two properties:

- $s_i \notin \mathrm{im}(\rho_{i-1,i})$;
- $\rho_{i,j-1}(s_i) \notin \mathrm{im}(\rho_{i-1,j-1})$ and $\rho_{i,j}(s_i) \in \mathrm{im}(\rho_{i-1,j})$,

where the death j may be ∞ if s_i is still alive at n.

As Edelsbrunner and Harer mentioned in [26], the s_i has death j if it merges with an older class in $H_q(X_{j-1})$. The following approximation lemma can be viewed as a local

version of barcodes of elements, which approximates the upper bound of deaths for any s_i, s_j who are coinciding at some k.

Lemma 2.2.1 (Approximation Lemma). *Let $\emptyset = X_0 \subseteq X_1 \subseteq \cdots \subseteq X_n$ be a filtration of topological spaces, $q \geq 0$, $0 \leq i < j$, $s_i \in H_q(X_i)$, and $s_j \in H_q(X_j)$ which has barcode (j, d). If s_i, s_j coincide at $k \geq j$, then $d \leq k$.*

Proof. We first note that k must be strictly larger than j: If $k = j$, then $s_j = \rho_{j,j}(s_j) = \rho_{i,j}(s_i) = (\rho_{j-1,j} \circ \rho_{i,j-1})(s_i)$, this shows that $s_j \in \mathrm{im}(\rho_{j-1,j})$ and contradicts to s_j is born at j. Hence we have $k > j$.

Suppose $d > k$, then $i < j < k \leq d-1$. In particular, s_j doesn't die at k. By definition of death, either $\rho_{j,k-1}(s_j) \in \mathrm{im}(\rho_{j-1,k-1})$ or $\rho_{j,k}(s_j) \notin \mathrm{im}(\rho_{j-1,k})$. Because

$$\rho_{j,k}(s_j) = \rho_{i,k}(s_i) = \rho_{j-1,k}(\rho_{i,j-1}(s_i)) \in \mathrm{im}(\rho_{j-1,k}),$$

we must have $\rho_{j,k-1}(s_j) \in \mathrm{im}(\rho_{j-1,k-1})$. Because $j \leq k-1 \leq d-1$, we have

$$\rho_{j,d-1}(s_j) = (\rho_{k-1,d-1} \circ \rho_{j,k-1})(s_j) \in \mathrm{im}(\rho_{j-1,d-1}) \tag{9}$$

since $\rho_{k-1,d-1}(\mathrm{im}(\rho_{j-1,k-1})) = \mathrm{im}(\rho_{j-1,d-1})$. However, $s_j \notin \mathrm{im}(\rho_{j-1,d-1})$ since s_j dies at d, a contradiction. This shows that $d \leq k$. □

The approximation lemma can be used for estimating whether a certain pair (s_i, s_j) coincides at some $k \geq \max\{i, j\}$ or not. To adapt the lemma, we say a filtration which is *short* if it has the form $\emptyset = X_0 \subseteq X_1 \subseteq X_2 \subseteq X_3$.

Theorem 2.2.2. *Let $\mathcal{F} : \emptyset = X_0 \subseteq X_1 \subseteq \cdots \subseteq X_n$ be a filtration of topological spaces, $q \geq 0$, $0 \leq i < j < k$, and $s_j \in H_q(X_j)$ which is born at j. Define short filtration*

$$\mathcal{G} : \emptyset = Y_0 \subseteq Y_1 \subseteq Y_2 \subseteq Y_3 \tag{10}$$

where $Y_0 = X_0$, $Y_1 = X_i$, $Y_2 = X_j$, and $Y_3 = X_k$, then s_j coincides to some $s_i \in H_q(X_i)$ at k in $\mathcal{F}$ if and only if $s_j \in H_q(Y_2)$ has barcode $(2, 3)$ in $\mathcal{G}$.

Proof. We first assume there is an $s_i \in H_q(X_i)$ such that s_i and s_j coincide at k in $\mathcal{F}$. Because s_j is born at j in $\mathcal{F}$, $\rho_{i,j}(s_i) \neq s_j$. Hence s_j is also born at 2 in $\mathcal{G}$. In $\mathcal{G}$, s_i and s_j also coincide at 3, by the approximation lemma, the death of s_j in must ≤ 3, and it forces that s_j has barcode $(2, 3)$ in $\mathcal{G}$.

Conversely, suppose $s_j \in H_q(Y_2)$ has barcode $(2, 3)$ in $\mathcal{G}$, then $\rho^{\mathcal{G}}_{2,3}(s_j) \in \mathrm{im}(\rho^{\mathcal{G}}_{1,3})$ where $\rho^{\mathcal{G}}_{\bullet,\bullet}$'s are the induced linear transformations from $\rho_{\bullet,\bullet}$ in $\mathcal{F}$. This shows that there is an $s_i \in H_q(Y_1) = H_q(X_i)$ such that $\rho_{i,k}(s_i) = \rho^{\mathcal{G}}_{1,3}(s_i) = \rho^{\mathcal{G}}_{2,3}(s_j) = \rho_{j,k}(s_j)$ i.e., s_i and s_j coincide at k in $\mathcal{F}$. □

2.3. Sheaf Structures on Binary Images

The subsection is separated into two parts. We first introduce some notations and terminologies for binary images, and then introduce the *short filtrations* for a single binary image and apply its sheaves to compute the local merging numbers.

Binary Images

A 2-dimensional *digital image* can be regarded as a function $f : S \to \mathbb{R}_{\geq 0}$, where S is a subset of the 2-dimensional grid $\mathbb{Z}^2$. Typically, $S = ([a, b] \times [c, d]) \cap \mathbb{Z}^2$ is a rectangle, called the set of pixels of image f [58, 60, 51]. A digital image is said to be *binary* if it has range $\{0, 1\}$ where 0 and 1 usually denote the pixel values of black and white respectively. The set of all black pixels in S is the pre-image set $f^{-1}(0)$.

By viewing every set of black pixels $f^{-1}(0) \subseteq \mathbb{Z}^2$ of a binary image $f : S \to \{0, 1\}$ as a collection of squares in $\mathbb{R}^2$ i.e., a *cubical complex* embedded in $\mathbb{R}^2$ [65, 38, 48, 63]. Because the union of squares can be viewed as a subspace of $\mathbb{R}^2$, the computation of homologies are valid.

For a 2-dimensional image f, the homology of $f^{-1}(0)$ detects the numbers (β_0, β_1) of connected components and 1-dimensioanl holes form by black pixels of f respectively, which are called the *Betti numbers* [33, 26]. More precisely, $\beta_q = \dim_{\mathbb{Z}_2} H_q(f^{-1}(0))$, $q = 0, 1$. For example, as (c) in Figure 1, if $f = g_3$ is the image "AI", then

$$\begin{aligned} H_0(f^{-1}(0)) &= \mathrm{span}_{\mathbb{Z}_2}\{\text{“A”}, \text{“I”}\}, \\ H_1(f^{-1}(0)) &= \mathrm{span}_{\mathbb{Z}_2}\{\text{“A”}\}. \end{aligned} \tag{11}$$

because "A" and "I" represent different connected components of "AI" and "A" contains a 1-dimensional hole. In particular, $\beta_0 = 2$ and $\beta_1 = 1$.

Cellular Sheaves on Single Binary Image

We propose a method for analyzing connecting relations between local objects in a binary image by using sheaf structure. Let X be a topological space and X_1, X_2 be subspaces of X. We imitate the idea in Theorem 2.1.3 to construct the natural cellular sheaf structure

$$\begin{array}{ccc} H_q(X_1) & \xrightarrow{\rho_1} & H_q(X) \\ & & \uparrow{\scriptstyle \rho_2} \\ & & H_q(X_2) \end{array} \tag{12}$$

where ρ_1, ρ_2 are induced by the inclusion maps. Now we have two short filtrations

$$\begin{aligned} \mathcal{G}_1 &: \emptyset \subseteq X_1 \subseteq X_1 \cup X_2 \subseteq X, \\ \mathcal{G}_2 &: \emptyset \subseteq X_2 \subseteq X_1 \cup X_2 \subseteq X. \end{aligned} \tag{13}$$

and persistent homologies

$$\begin{aligned} 0 \to H_q(X_1) \xrightarrow{\omega_1} H_q(X_1 \cup X_2) \xrightarrow{\gamma} H_q(X), \\ 0 \to H_q(X_2) \xrightarrow{\omega_2} H_q(X_1 \cup X_2) \xrightarrow{\gamma} H_q(X), \end{aligned} \tag{14}$$

whenever $q \geq 0$, where ω_1, ω_2 and γ are induced by the inclusion maps and $\gamma \circ \omega_i = \rho_i$ for $i = 1, 2$.

In addition, when $\mathrm{cl}_X(X_1)$ and $\mathrm{cl}_X(X_2)$ are disjoint[6], the canonical mapping

$$\omega_1 + \omega_2 : H_q(X_1) \oplus H_q(X_2) \to H_q(X_1 \cup X_2) \tag{15}$$

defined by $(\xi_1, \xi_2) \longmapsto \xi_1 + \xi_2$ is an isomorphism ([33] Proposition (9.5)). In this case, ω_1 and ω_2 in (14) are one-to-one. Because $\omega_1 + \omega_2$ is bijective, every element s in $H_q(X_1 \cup X_2)$ can be uniquely represented by $s_1 + s_2$, where $s_i = \omega_i(\widetilde{s_i})$ for some $\widetilde{s_i} \in H_q(X_i)$, $i = 1, 2$. In particular, we have the following theorem.

Theorem 2.3.1. *Let X, X_1, X_2, $q \geq 0$ and ρ_i, ω_i, γ, $i = 1, 2$ be defined as above. If $\mathrm{cl}_X(X_1) \cap \mathrm{cl}_X(X_2) = \emptyset$, then the following hold:*

(a) *The persistence diagram $\mathcal{P}_q(\mathcal{G}_1)$ has no barcodes of birth $= 2$ if and only if $H_q(X_2) = \{0\}$.*

(b) *For $s_2 = \omega_2(\widetilde{s_2}) \in H_q(X_1 \cup X_2)$, $s_2 \neq 0$ if and only if it is born at 2 in $\mathcal{G}_1$.*

(c) *For non-zero $\widetilde{s_2} \in H_q(X_2)$, $(\widetilde{s_1}, \widetilde{s_2}) \in H_q(X_1) \oplus H_q(X_2)$ is a local section in (12) for some $\widetilde{s_1} \in H_q(X_1)$ if and only if $s_2 := \omega_2(\widetilde{s_2})$ has barcode $(2, 3)$ in $\mathcal{G}_1$.*

Proof. (a) Because $\omega_1 + \omega_2$ is an isomorphism, $P_q(\mathcal{G}_1)$ has not barcodes of birth $= 2$ if and only if $\mathrm{im}(\omega_1) = H_q(X_1 \cup X_2) = \mathrm{im}(\omega_1 + \omega_2)$ if and only if ω_2 is the zero map if and only if $H_q(X_2) = \{0\}$ (since w_2 is one-to-one).

(b) The converse direction is trivial. If $s_2 = \omega_2(\widetilde{s_2}) = (\omega_1 + \omega_2)(0, \widetilde{s_2})$ is non-zero, then $s_2 \notin \mathrm{im}(\omega_1) = \mathrm{im}(\omega_1 + \omega_2)$ since $\omega_1 + \omega_2$ is one-to-one.

(c) By (b), s_2 is born at 2 since $\widetilde{s_2} \neq 0$ and ω_2 is one-to-one. To adapt Theorem 2.2.2, it is sufficient to note that $\rho_1(\widetilde{s_1}) = s_2$ if and only if $\gamma(\omega_1(\widetilde{s_1})) = s_2$ i.e., $\widetilde{s_1}$ and s_2 coincide at 3 in $\mathcal{G}_1$. Now (c) follows from Theorem 2.2.2 immediately. □

As in Figure 5, the 0-dimensional PD $\mathcal{P}_0(\mathcal{G}_1)$ of $\mathscr{G}_1$ is the multiset $\{(1, +\infty), (2, 3), (2, 3)\}$ while $\mathcal{P}_0(\mathcal{G}_2) = \{(1, +\infty), (2, 3)\}$. It indicates that the space X_1 has two merging parts in X. From the X_2's point of view, it has single merging part since X_1 is the unique component in X which connects to X_2. Now the following definitions can be established:

[6]If X is a topological space and A is a subset of X, $\mathrm{cl}_X(A)$ denotes the closure of A in X.

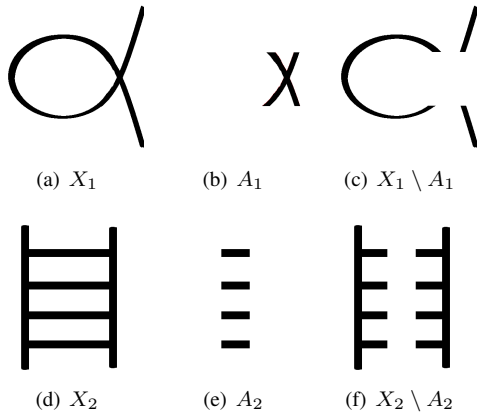

(a) X_1 (b) A_1 (c) $X_1 \setminus A_1$

(d) X_2 (e) A_2 (f) $X_2 \setminus A_2$

Figure 4. Examples of spaces $X_1, X_2 \subseteq \mathbb{R}^2$ and their subspaces A_1, A_2. Then $\beta_0(X_1 \setminus A_1) - \beta_0(X_1) + \beta_0(A_1) = 3 - 1 + 1 = 3$ and $\beta_0(X_2 \setminus A_2) - \beta_0(X_2) + \beta_0(A_2) = 2 - 1 + 4 = 5$.

Definition. *Let X, X_1, X_2, and $\mathcal{G}_1, \mathcal{G}_2$, $i = 1, 2$ be defined as in Theorem 2.3.1, then the q^{th} **local merging number** of X_1 with respect to X_2 in X is defined as the number of barcodes $(2, 3)$ in the multiset $\mathcal{P}_q(\mathcal{G}_1)$, denoted by $m_q(X_1; X_2)$.*

We describe the main differences between local merging and local branch numbers ([64]). Take Figure 4 as an illustrative example. Based on [64], the local branch number of A_1 in Figure 4 is 4 since the graph which fits A_1 has four vertices in degree 1. On the other hand, the local merging number of A_1 in Figure 4 is 3 as demonstrated in Figure 7 (g)-(i). As shown in Figure 4 (c), there are three connected components of $X_1 \setminus A_1$ that connect to A_1. Another difference is that the local branch numbers are constructed from Vietoris-Rips complexes on the point cloud data. Therefore, tuning parameters such as sampling the points, and choosing the radius would be a critical step [64]. On the other hand, our local merging numbers are purely dependent on the choices of $X_1, X_2 \subseteq X$ and can be exactly computed by the cellular sheaf structures. Branches and merging relations base on different geometric aspects, we thought both features are important for describing the connection between global and local objects.

Definition. *A **system of patches** of a topological space X is a (finite) collection of pairs $(X_1^{(i)}, X_2^{(i)})$'s of subspaces of X such that $\mathrm{cl}_X(X_1^{(i)}) \cap \mathrm{cl}_X(X_2^{(i)}) = \emptyset$ for every i.*

Remark. *As shown in Figure 4 (a)-(c), it may suggest that the 0^{th} local merging number of $A \subseteq X$ as*

$$\beta_0(X \setminus A) - \beta_0(X) + \beta_0(A). \tag{16}$$

This is the special case when $\beta_0(A) = 1$. In general, this formula (16) would not hold. For example, in Figure 4 (d)-(f), $\beta_0(X_2 \setminus A_2) - \beta_0(X_2) + \beta_0(A_2)$ equals 5 while the local

(a) X (b) X_1 (c) X_2 (d) $X_1 \cup X_2$

Figure 5. An example of spaces X in $\mathbb{R}^2$ and its subspaces X_1, X_2, which satisfy $\mathrm{cl}_X(X_1) \cap \mathrm{cl}_X(X_2) = \emptyset$.

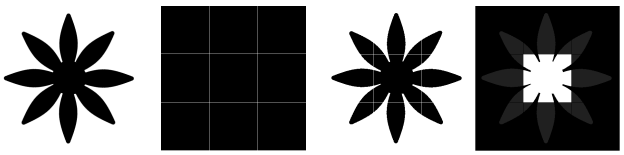

(a) Input image (b) Windows (c) $\{X_1^{(i)}\}_{i=1}^9$ (d) Merging numbers

Figure 6. An example of windows, patches and merging numbers.

merging number of A_2 is 2. It shows that there are exactly two connected components in X_2 that connect to A_2 and gives us more explainable information than the number 5.

3. Demonstration

In the section, we demonstrate how do we use the proposed method to automatically detect local merging numbers of a binary image. The demonstration aims to automatically generated a heat map $m_0(f)$ for representing local merging numbers of local regions of a binary image $f : S \to \{0, 1\}$ where $S = ([a, b] \times [c, d]) \cap \mathbb{Z}^2$. Clearly, the $m_0(f)$ depends on how do we define patches $\{(X_1^{(i)}, X_2^{(i)})\}_{i=1}^n$ of $f^{-1}(0)$, hence $m_0(f)$ is not unique.

To construct a system of patches of a binary image, for each local window $S' := ([a', b'] \times [c', d']) \cap \mathbb{Z}^2$ with $a \le a' \le b' \le b$ and $c \le c' \le d' \le d$, we define $\widehat{X_1} = f^{-1}(0) \cap S'$ and $X_2 = f^{-1}(0) \setminus \widehat{X_1}$. Next, we define

$$X_1 = \widehat{X_1} \setminus \{(x, y) \in \widehat{X_1} : x = a' \text{ or } y = b'\}. \tag{17}$$

In other words, we obtain X_1 by removing all black pixels which belong to the boundary of S'. Because finite cubic complexes in $\mathbb{R}^2$ are finite unions of closed $\mathbb{R}^2$-squares, they are closed in $\mathbb{R}^2$ (and so do X). Hence we must have $\mathrm{cl}_X(X_1) \cap \mathrm{cl}_X(X_2) = \emptyset$.

For example, as in Figure 6, if we consider local windows in (b), then for image (a), the family $\{X_1^{(i)}\}_{i=1}^9$ of black pixels in (c) induces a system of patches $\{(X_1^{(i)}, X_2^{(i)})\}_{i=1}^9$, and (d) is the corresponding heat map of local merging numbers. The heat map (d) corresponds to

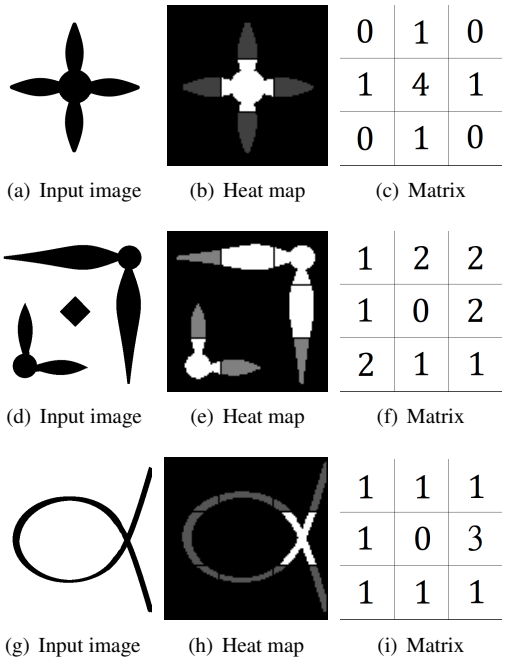

(a) Input image (b) Heat map (c) Matrix

(d) Input image (e) Heat map (f) Matrix

(g) Input image (h) Heat map (i) Matrix

Figure 7. More examples of images, heat maps, and matrices.

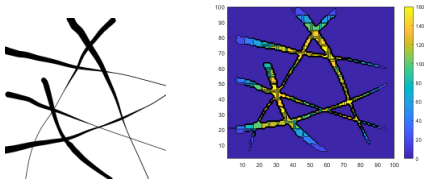

(a) Input image (b) Heat map

Figure 8. Image and its heat map of local merging numbers. Local parts with more complicated structures may have higher merging numbers (*e.g.* cross parts, corners or cusps).

the matrix

$$\begin{array}{|c|c|c|}\hline 1 & 1 & 1 \\ \hline 1 & 8 & 1 \\ \hline 1 & 1 & 1 \\ \hline \end{array} \tag{18}$$

of local merging numbers. The black pixels separated by the central window have a merging number 8 since there are 8 fans connect to the central object. Other fans have the same merging number 1 since only one connected object connects to each fan. With the same windows in Figure 6 (b), we provide more heat maps and corresponding matrices of squared images as examples for explaining our method. Every image was resized into 100×100 pixels, and its heat map can be generated in nearly 5 seconds[7].

Alternatively, we can also apply the sliding window al-

[7]Local merging numbers are invariant under the transformation of similar objects in $\mathbb{R}^2$.

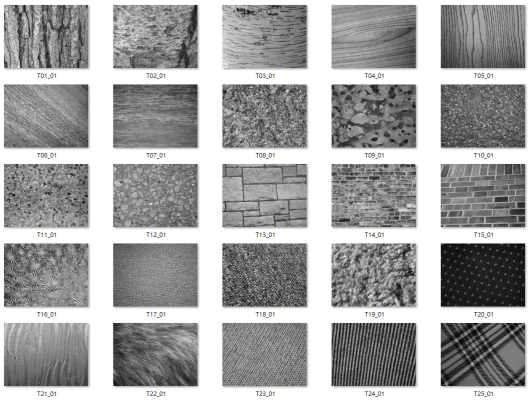

(a) Selected Images in UIUC

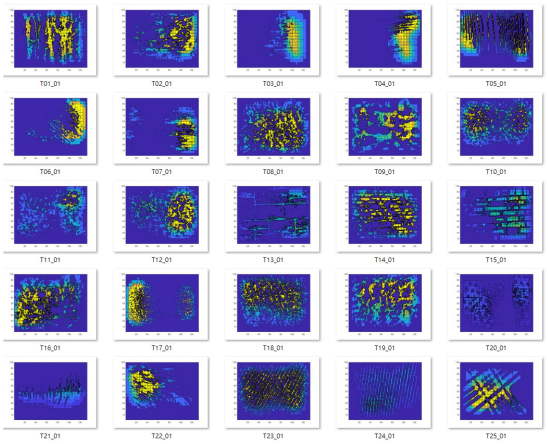

(b) Heat maps of merging numbers of selected Images

Figure 9. Images in UIUC dataset and their heat maps.

gorithm [12] to compute the local merging numbers of local windows. In the demonstration, we unify each binary image f to have size of 100×100 pixels, and consider three local windows of sizes 10×10, 20×20, and 30×30. For each local window we obtain heat map $m_0^n(f)$, $n = 10, 20, 30$, and finally output $m_0(f)$ as the sum of all $m_0^n(f)$'s. Figure 8 and Figure 9 are examples. The codes of the demonstration were run by `Matlab 2020b` based on `Windows 10`, and the PDs were computed by the software `Perseus` [52].

4. Discussion and Conclusion

Based on our investigation, the proposed work is the first one that combines sheaf structures and persistence diagrams to capture the local merging numbers of binary images. We use the simplest sheaf structure (6) to derive the merging relation between pairs of local objects. One future direction is to investigate the meaning and applications of local sections of homologies in $q \geq 1$, and consider more complicated sheaf structures, such as the coincidence of n-tuples $(s_1, ..., s_n)$ and their topological insights behind the algebraic coincidence.

Although the form of the diagram (6) is the simplest form of the zigzag homology [20, 57], multi-parameter persistent homology [20, 57], and cellular sheaf [24, 55, 54], the fruitful tools developed in the theories were not considered in the work, such as cellular sheaf cohomology and multi-persistence. Analyzing digital images by combining these advanced tools is also a future direction.

We also demonstrate our method on UIUC dataset [45] in Figure 9, which is a well-known dataset in texture classification task [41]. The UIUC dataset provides 25 classes of images in different textures. We select one image per class and compute its heat map, where we transform each image to a binary one by setting its average pixel value as a threshold. The result shows that images in different classes have different characteristics of heat maps. For example, heat maps of textures with regular patterns may distribute more uniformly, and heat maps of natural textures (*e.g.* wood surfaces) may contain small and non-regular pieces that have high $m_0(f)$. As a low-level feature, the local merging numbers may provide useful information in certain image classification tasks.

Lastly, since the local merging numbers provide a heat map of an image, it can be viewed as a natural attention map. Local parts that have higher local merging values show that they are the joint areas crossed by different objects, and might be important in some image analysis tasks (*e.g.* medical images). Because every image and its heat map have the same size, the latter one can be viewed as an additional channel of an image input in neural network models (*e.g.* AlexNet [43] or ResNet [37]). We also plan to integrate this geometrically explainable feature into current DNN models for some computer vision tasks.

To conclude this paper, we highlight our contribution. We proposed a new theory to generate the local merging numbers in a binary image by using cellular sheaves on short persistent homology. Moreover, the approximation theorem shows that local sections in cellular sheaves can be computed via barcodes in persistence diagrams of short filtrations. Because the local merging numbers are purely provided by the intrinsic geometry of the given image, no learning procedures needed in the method. We also implemented the code for generating local merging numbers, which has the potential to be integrated into DNN models.

Acknowledgements

Chuan-Shen Hu is supported by the projects MOST 107-2115-M-003-012-MY2, MOST 108-2119-M-002-031, and MOST 108-2115-M-003-005-MY2 hosted by the Ministry of Science and Technology in Taiwan.

References

[1] Henry Adams, Tegan Emerson, Michael Kirby, Rachel Neville, Chris Peterson, Patrick Shipman, Sofya Chepushtanova, Eric Hanson, Francis Motta, and Lori Ziegelmeier. Persistence images: A stable vector representation of persistent homology. *Journal of Machine Learning Research*, 18(8):1–35, 2017. 1

[2] Paul Alexandroff. Über den allgemeinen dimensionsbegriff und seine beziehungen zur elementaren geometrischen anschauung. *Mathematische Annalen*, 1928. 2

[3] Pavel Alexandroff. *Diskrete räume*. Mat. Sb, 2:501-518, 1937. 2, 3

[4] Pavel Alexandrov. *Combinatorial Topology*. Dover Publications, Inc., 31 East 2nd Street, Mineola, NY, 1947. 2, 3

[5] D Vijay Anand, Zhenyu Meng, Kelin Xia, and Yuguang Mu. Weighted persistent homology for osmolyte molecular aggregation and hydrogen-bonding network analysis. *Scientific Reports*, 10:9685, 06 2020. 1

[6] Ulrich Bauer, Michael Kerber, Jan Reininghaus, and Hubert Wagner. Phat - persistent homology algorithms toolbox. *J. Symb. Comput.*, 78:76–90, 2017. 1

[7] Paul Bendich, James Marron, Ezra Miller, Alex Pieloch, and Sean Skwerer. Persistent homology analysis of brain artery trees. *Arxiv*, 2014. 1

[8] Nicolas Berkouk. *Persistence and Sheaves : from Theory to Applications*. Theses, Institut Polytechnique de Paris, Sept. 2020. 2

[9] Alexander Bernstein, Evgeny Burnaev, Maxim Sharaev, Ekaterina Kondrateva, and Oleg Kachan. Topological data analysis in computer vision. In *Twelfth International Conference on Machine Vision (ICMV)*, page 140, 01 2020. 1

[10] Christophe Biscio and Jesper Møller. The accumulated persistence function, a new useful functional summary statistic for topological data analysis, with a view to brain artery trees and spatial point process applications. *Journal of Computational and Graphical Statistics*, 28:671 – 681, 2016. 1

[11] Holger Boche, Mijail Guillemard, Gitta Kutyniok, and Friedrich Philipp. Signal analysis with frame theory and persistent homology. *The Conference of Sampling Theory and Applications, SampTA'13*, 01 2013. 1

[12] Vladimir Braverman. *Sliding Window Algorithms*, pages 2006–2011. Springer New York, New York, NY, 2016. 8

[13] Glen Bredon. *Sheaf Theory*. Graduate Texts in Mathematics. Springer New York, 1997. 2, 3

[14] Peter Bubenik. Statistical topological data analysis using persistence landscapes. *Journal of Machine Learning Research*, 16(3):77–102, 2015. 1

[15] Gunnar Carlsson. Topology and data. *Bulletin of the American Mathematical Society*, 46(2):255–308, 2009. 1

[16] Gunnar Carlsson and Vin de Silva. Zigzag persistence. *Arxiv*, 2008. 2

[17] Gunnar Carlsson, Vin de Silva, Sara Kališnik, and Dmitriy Morozov. Parametrized homology via zigzag persistence. *Algebr. Geom. Topol.*, 19(2):657–700, 2019. 2

[18] Gunnar Carlsson, Anjan Dwaraknath, and Bradley Nelson. Persistent and zigzag homology: A matrix factorization viewpoint. *Arxiv*, 2019. 2

[19] Gunnar Carlsson, Vin De Silva, and Dmitriy Morozov. Zigzag persistent homology and real-valued functions. In *In Proceedings of the 25th ACM Symposium on Computational Geometry*, 2009. 2

[20] Gunnar Carlsson, Gurjeet Singh, and Afra Zomorodian. Computing multidimensional persistence. In *Algorithms and Computation*, pages 730–739, Berlin, Heidelberg, 2009. Springer Berlin Heidelberg. 2, 8

[21] Gunnar Carlsson, Afra Zomorodian, Anne Collins, and Leonidas Guibas. Persistence barcodes for shapes. *International Journal of Shape Modeling*, 11:149–188, 01 2005. 1

[22] Moo Chung, Jamie Hanson, Jieping Ye, Richard Davidson, and Seth Pollak. Persistent homology in sparse regression and its application to brain morphometry. *IEEE transactions on medical imaging*, 34, 08 2014. 1

[23] Justin Curry. *Sheaves, Cosheaves and Applications*. PhD Thesis, 2014. 3

[24] Justin Curry. Topological data analysis and cosheaves. *Japan Journal of Industrial and Applied Mathematics*, 2015. 2, 3, 8

[25] Herbert Edelsbrunner. Persistent homology: theory and practice. *Bulletin of the American Mathematical Society*, 2014. 1

[26] Herbert Edelsbrunner and John Harer. *Computational Topology: An Introduction*. American Mathematical Society, 01 2010. 1, 4, 5

[27] Herbert Edelsbrunner, David Letscher, and Afra Zomorodian. Topological persistence and simplification. *Discrete Comput Geom*, 28:511–533, 2002. 1

[28] Samuel Eilenberg and Norman Steenrod. *Foundations of Algebraic Topology*. Foundations of Algebraic Topology. Princeton University Press, 1952. 2

[29] Brittany Fasy and Bei Wang. Exploring persistent local homology in topological data analysis. In *2016 IEEE International Conference on Acoustics, Speech and Signal Processing (ICASSP)*, pages 6430–6434, 03 2016. 2

[30] Brittany Fasy and Carola Wenk. Local persistent homology based distance between maps. In *the 22nd ACM SIGSPATIAL International Conference*, pages 43–52, 11 2014. 2

[31] Robert Ghrist. *Elementary Applied Topology*. CreateSpace Independent Publishing Platform, 2014. 2

[32] Robert Ghrist and Hans Riess. Cellular sheaves of lattices and the tarski laplacian. *Arxiv*, 2020. 3

[33] Marvin Greenberg and John Harper. *Algebraic Topology, A First Course*. Addison-Wesley Publishing Company, 1980. 4, 5, 6

[34] Jakob Hansen and Robert Ghrist. Opinion dynamics on discourse sheaves. *Arxiv*, 2020. 2

[35] Heather Harrington, Nina Otter, Hal Schenck, and Ulrike Tillmann. Stratifying multiparameter persistent homology. *Arxiv*, 2019. 2

[36] Robin Hartshorne. *Algebraic Geometry*. Springer-Verlag, New York, 1977. 2, 3

[37] Kaiming He, Xiangyu Zhang, Shaoqing Ren, and Jian Sun. Deep residual learning for image recognition. In *2016 IEEE Conference on Computer Vision and Pattern Recognition (CVPR)*, pages 770–778, 2016. 8

[38] Tomasz Kaczynski, Konstantin Mischaikow, and Marian Mrozek. *Computational Homology*. Applied Mathematical Sciences. Springer New York, 2004. 5

[39] Masaki Kashiwara and Pierre Schapira. Persistent homology and microlocal sheaf theory. *Journal of Applied and Computational Topology*, 2, 10 2018. 2

[40] Masaki Kashiwara and Pierre Schapira. Piecewise Linear Sheaves. *International Mathematics Research Notices*, 08 2019. rnz145. 2

[41] Soheil Kolouri, Yang Zou, and Gustavo Rohde. Sliced wasserstein kernels for probability distributions. In *IEEE Conference on Computer Vision and Pattern Recognition (CVPR)*, pages 5258–5267, 06 2016. 8

[42] Rami Kraft. *Illustrations of Data Analysis Using the Mapper Algorithm and Persistent Homology*. TRITA-MAT-E. Master Thesis, 2016. 2

[43] Alex Krizhevsky, Ilya Sutskever, and Geoffrey Hinton. Imagenet classification with deep convolutional neural networks. In F. Pereira, C. J. C. Burges, L. Bottou, and K. Q. Weinberger, editors, *Advances in Neural Information Processing Systems*, volume 25, pages 1097–1105. Curran Associates, Inc., 2012. 8

[44] Genki Kusano, Kenji Fukumizu, and Yasuaki Hiraoka. Kernel method for persistence diagrams via kernel embedding and weight factor. *Journal of Machine Learning Research*, 18(189):1–41, 2018. 1

[45] Svetlana Lazebnik, Cordelia Schmid, and Jean Ponce. A sparse texture representation using local affine regions. *IEEE Transactions on Pattern Analysis and Machine Intelligence*, 27(8):1265–1278, 2005. 8

[46] Hyekyoung Lee, Hyejin Kang, Moo Chung, Bung-Nyun Kim, and Dong Soo Lee. Persistent brain network homology from the perspective of dendrogram. *IEEE Transactions on Medical Imaging*, 31(12):2267–2277, 2012. 1

[47] Qing Liu. *Algebraic Geometry and Arithmetic Curves*. Oxford Graduate Texts in Mathematics, 2006. 2, 3

[48] Clément Maria. Filtered complexes. In *GUDHI User and Reference Manual*. GUDHI Editorial Board, 3.1.1 edition, 2020. 5

[49] Clément Maria, Jean-Daniel Boissonnat, Marc Glisse, and Mariette Yvinec. The gudhi library: Simplicial complexes and persistent homology. In *Mathematical Software – ICMS 2014*, pages 167–174, Berlin, Heidelberg, 2014. Springer Berlin Heidelberg. 1

[50] Gabriell Máté, Andreas Hofmann, Nicolas Wenzel, and Dieter Heermann. A topological similarity measure for proteins. *Biochimica et Biophysica Acta (BBA) - Biomembranes*, 1838(4):1180 – 1190, 2014. Viral Membrane Proteins - Channels for Cellular Networking. 1

[51] Laurent Najman and Hugues Talbot. *Mathematical Morphology*. Wiley-ISTE, 1d edition, 2010. 5

[52] Vidit Nanda. Perseus, the persistent homology software. `http://www.sas.upenn.edu/~vnanda/perseus`, 2013. 8

[53] Chi Seng Pun, Kelin Xia, and Si Xian Lee. Persistent-homology-based machine learning and its applications – a survey. *Arxiv*, 2018. 1

[54] Michael Robinson. The nyquist theorem for cellular sheaves. *Sampling Theory and Applications 2013, Bremen, Germany*, 2013. 2, 3, 8

[55] Michael Robinson. *Topological Signal Processing*. Mathematical Engineering. Springer Berlin Heidelberg, 2014. 2, 3, 8

[56] Michael Robinson. Hunting for foxes with sheaves. *Notices of the American Mathematical Society*, page 661, 05 2019. 2, 3

[57] Sara Scaramuccia, Federico Iuricich, Leila De Floriani, and Claudia Landi. Computing multiparameter persistent homology through a discrete morse-based approach. *Computational Geometry*, 89:101623, 2020. 2, 8

[58] Jean Serra. *Image Analysis and Mathematical Morphology*. Number 1 in Image Analysis and Mathematical Morphology. Academic Press, 1984. 5

[59] Gurjeet Singh, Facundo Mémoli, and Gunnar Carlsson. Topological methods for the analysis of high dimensional data sets and 3d object recognition. In *PBG@Eurographics*, 2007. 2

[60] Pierre Soille. *Morphological Image Analysis: Principles and Applications*. Springer-Verlag New York, Inc., Secaucus, NJ, USA, 2 edition, 2003. 5

[61] Anirudh Som, Hongjun Choi, Karthikeyan Natesan Ramamurthy, Matthew Buman, and Pavan Turaga. Pi-net: A deep learning approach to extract topological persistence images. *CoRR*, abs/1906.01769, 2019. 1

[62] Daniel Spitz, Jürgen Berges, Markus Oberthaler, and Anna Wienhard. Finding universal structures in quantum many-body dynamics via persistent homology. *Arxiv*, 2020. 1

[63] The GUDHI Project. *GUDHI User and Reference Manual*. GUDHI Editorial Board, 3.1.1 edition, 2020. 5

[64] Robin Vandaele, Tijl De Bie, and Yvan Saeys. Local topological data analysis to uncover the global structure of data approaching graph-structured topologies. In *Machine Learning and Knowledge Discovery in Databases*, pages 19–36, Cham, 2019. Springer International Publishing. 2, 6

[65] Hubert Wagner, Chao Chen, and Erald Vuçini. *Efficient Computation of Persistent Homology for Cubical Data*. Springer Berlin Heidelberg, Berlin, Heidelberg, 2012. 5

[66] Zhichao Wang, Qian Li, Gang Li, and Guandong Xu. Polynomial representation for persistence diagram. In *2019 IEEE/CVF Conference on Computer Vision and Pattern Recognition (CVPR)*, pages 6116–6125, 2019. 1

[67] Xiaojin Zhu. Persistent homology: An introduction and a new text representation for natural language processing. *IJCAI International Joint Conference on Artificial Intelligence*, pages 1953–1959, 08 2013. 1